

# Compact waveguide circulator based on T-shaped magneto-photonic crystal pillar array

YONG WANG<sup>a</sup>, DENG GUO ZHANG<sup>b,\*</sup>, SHIXIANG XU<sup>b</sup>, BIAOGANG XU<sup>b</sup>, ZHENG DONG<sup>b</sup>, TAN HUANG<sup>b</sup>

<sup>a</sup>College of Optoelectric Engineering, Shenzhen University, Shenzhen, China, 518060

<sup>b</sup>College of Electronic Science and Technology, Shenzhen University, Shenzhen, China, 518060

A T-shaped defect structure based on two-dimensional square-lattice magneto-photonic pillar array is proposed and a novel compact waveguide circulator using cylindrical ferrite rods is numerically investigated. Under a bias DC magnetic field, the ferrite rod in the central point of defect structure can provide Faraday rotation. External characteristics of the circulator are calculated by finite element method and the numerical results show that the isolation is 25.92dB and insertion loss is 0.064dB. Furthermore, according to the scaling theory of Maxwell's equations, a 3 cm T-junction circulator is developed by scaling the radius of the central ferrite cylinder.

(Received March 16, 2017; accepted June 7, 2018)

**Keywords:** Photonic crystal, Photonic device, Circulator, Ferrite, Optical integrated circuits

## 1. Introduction

Photonic crystals, a new class of artificial structures made of periodic dielectric materials, was first proposed in 1987 [1, 2]. Photonic crystals have been confirmed as an effective way to design optical integrated devices. An ultra-compact photonic crystal splitter is proposed by G. Shen et al and a slow-light waveguide for a microwave photonic filter is investigated [3]. A new angular selective filter is designed by J. G. Mutitu et al based on photonic band gap [4]. A compact thermo-optic switch is demonstrated by Q. Zhao et al with an integrated micro-heater using photonic crystal waveguide [5]. M. G. Scullion et al investigate high efficiency interface for coupling into slotted photonic crystal waveguides [6]. Photonic crystal integrated circuit as one of the most promising candidates to realize all-optical integrated chip, has become the focus of current research in integrate optical and optical communication [7-10].

Magneto-photonic crystal (MPC) circulators, as one kind of nonreciprocal passive device, have been studied in optical wavelengths [11] and terahertz band [12]. This device can be used to isolate the reflected light between adjacent devices or modules, in order to reduce interference and enhance the stability of large scale integrated optical circuit [13-17]. Due to the special property that wave can transmission in forward direction but isolation in reverse direction, circulator is widely used in high-resolution radar, radio astronomy and high speed data communications systems.

In this short paper, we will focus on developing an integrated conveniently circulator based on a T-shaped two-dimensional (2D) MPC waveguides. Moreover, the designed circulator's external parameters with frequency variation will be discussed. Furthermore, a 3 cm

T-junction 2D MPC circulator is investigated by scaling the radius of the central ferrite post, according to the scaling theory of Maxwell's equations.

## 2. Theoretical analysis

### 2.1. Properties of the gyromagnetic ferrite in microwave band

The saturated magnetized ferrite under an external DC magnetic field in the z-axis direction is a gyromagnetic material. In microwave band, the gyromagnetic characteristic of which can be expressed as permeability tensor in the following form:

$$\vec{\mu} = \begin{bmatrix} \mu_r & j\kappa & 0 \\ -j\kappa & \mu_r & 0 \\ 0 & 0 & \mu_0 \end{bmatrix} \quad (1)$$

The elements of permeability tensor using Hilbert type are given by [17]:

$$\mu_r = \mu_0 \{1 + \omega_m (\omega_0 + i\alpha\omega) / [(\omega_0 + i\alpha\omega)^2 - \omega^2]\} \quad (2)$$

$$\kappa = \mu_0 \omega_m \omega / [(\omega_0 + i\alpha\omega)^2 - \omega^2] \quad (3)$$

where  $\omega_0 = \mu_0 \gamma H_0$ ,  $\omega_m = \mu_0 \gamma M_s$ ,  $\gamma = |e/m| = 1.759 \times 10^{11}$  C/kg is gyromagnetic ratio and  $M_s = 2.39 \times 10^5$  A/m is saturation magnetization of ferrite,  $\mu_0$  is the permeability in the vacuum,  $\omega$  is the frequency of the incident wave, and  $H_0$  is the external magnetic field strength. In the case of considering material with loss,  $\mu_r$  and  $\kappa$  are plural form here and loss coefficient is  $\alpha = 3 \times 10^{-5}$ . When loss coefficient is  $\alpha = 0$ , formulas (2)-(3) are shown in literature [17], in which circulator using gyrotropic Al-Ni-Zn ferrite post operates

in millimeter wave band. The symbol of off-diagonal element  $\kappa$  is decided by the direction of external DC magnetic field and the strength of Faraday gyromagnetic effect is measured by the quality factor  $Q = \kappa/\mu_r$ .

## 2.2. Structure of 2D MPC circulator

Several kinds of circulator using MPC defect structures have been reported in the literature [11-13]. A

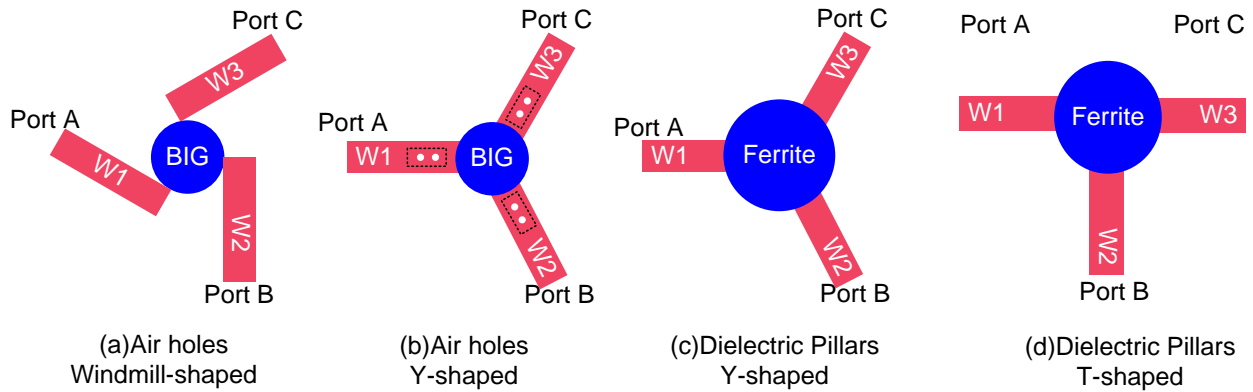


Fig. 1. Structures of 2D-MPCs circulator: (a) Air hole windmill shaped; (b) Air hole Y shaped; (c) Dielectric cylinder T shaped; (d) Dielectric cylinder cross-shaped

A new simpler 2D MPC defect structure is proposed to realize a T-shaped circulator in centimeter wave band by introducing a gyromagnetic ferrite post located at the center of the square-lattice pillar array. This ferrite post has a bigger radius  $r_2$  and labeled blue, shown in Fig. 2. Under the external DC magnetic field, not only does the ferrite post play a role of resonator, but also provide Faraday rotation effect. In order to improve the isolation of the circulator, two auxiliary rotation ferrite posts (blue) with smaller radius  $r_1 = 1.029 r_0$  are inserted in the square-lattice pillar array (red) around the center ferrite post, the detail structure in perspective, as shown in Fig. 2(b). Here, three line defects constitute standard T-shaped waveguides, which is integrated conveniently in large scale integrated optical circuit. Because of the waveguides adjacent to with the cavity, there is no need to add other smaller point defects within the waveguides in the dashed box at Fig. 1(b) to enhance the coupling efficiency. Therefore, the whole waveguides has no other defect structure and the amplitude of signal will be more stable. This arrangement can greatly reduce the insertion loss due to the multiple ferrite posts and lager point defect in the center compare with literature [18]. In microwave band, the testable circulator model is conceived by inserting 2D MPC pillar array in a metal (brass) case and designing three Flange interfaces, as shown in Fig. 2(c).

MPC structure is a heterogeneous medium. For an inhomogeneous system including gyromagnetic material, the form of the Maxwell equation can be expressed as

windmill shaped optical circulator based on air hole array has been studied by using FDTD method and perturbation method, shown in Fig. 1(a). The same as the former, air holes array distributed in magneto-optical materials (BIG) has been used to constitute a standard  $120^\circ$  Y-shaped circulator, shown in Fig. 1(b). In the terahertz band, a Y-shaped circulator using triangular lattice pillar array has been studied, as shown in Fig. 1(c).

following:

$$\nabla \times (\vec{\mu}^{-1} \cdot \nabla \times \vec{E}) - \varepsilon \cdot (\omega^2/c^2 \cdot \vec{E}) = 0 \quad (4)$$

where  $\varepsilon$  is the relative dielectric constant of MPC material, while  $\vec{\mu}$  is a function of space position. Transverse electric (TE) wave ( $E_x = 0, E_y = 0, E_z \neq 0$ ) will be discussed in detail in MPC structure. Because the magnetic field of transverse magnetic (TM) wave does not interact with the magnetic dipoles of the ferrite, the permeability for TM wave can be consider as a scalar of  $\mu_0$ . The magnetic field of TE wave interacts with the magnetic dipoles of the ferrite, so the permeability for TE wave in MPC structures is a tensor. And we will calculate the magnetic file by finite element method (FEM), which can be used for anisotropic mediums. We can substitute the parameters into the function of off-diagonal element  $\kappa$  and on-diagonal element  $\mu_r$  for our following simulation.

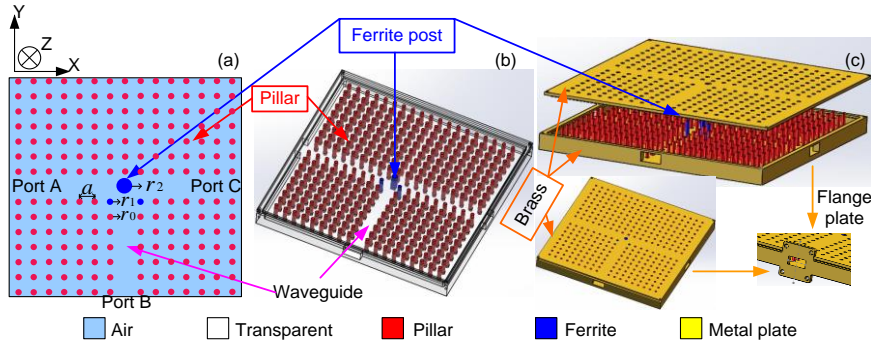


Fig. 2. (a) Defect structure with inserting ferrite posts; (b) T-shaped waveguides with transparent case for MPCs circulator; (c) Image of testable circulator model

### 2.3. Mode field analysis of ferrite post

In the electromagnetic theory, any cylinder surrounded by media of different refractive index, can be considered as cylindrical cavity with appropriate boundary. In this calculation, the boundary conditions use scattering boundary conditions (SBC) and the air around ferrite cylinder can consider as infinite. The modes of the cylindrical resonator are calculated by finite element method without any external magnetic field, show in Fig. 3, where the radius of the center ferrite post is  $r_2 = 1.6 r_0$ .

Numerical results shown that the cylinder resonator can support a pair of dipole degenerate modes with the same center normalized frequency  $a/\lambda = 0.4132$  in literature [18], as odd mode  $|o\rangle$  and even mode  $|e\rangle$ , shown in Figs. 3(a) and 3(b), respectively. The polarization direction of the two modes is mutually perpendicular represented by orange imaginary lines, shown in Fig. 3, respectively. When a DC magnetic field along the z-axis direction is applied on the magneto-optical material, coupling between the modes  $|e\rangle$  and  $|o\rangle$  takes place.

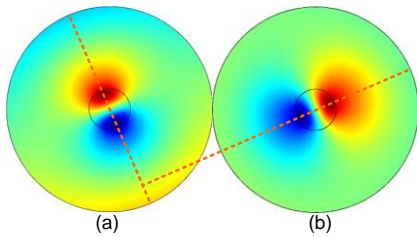


Fig. 3.  $E_z$  field distribution for the doubly degenerate modes in micro-cavity formed by a point defect: (a) Odd mode; (b) Even mode

## 3. Numerical demonstrations of circulator

### 3.1. TE band structure

In the absence of external magnetic field, the band gap of TE model structure will be calculated by plane wave expansion (PWE) method in square lattice pillar array. In order to make the numerical results more accurate and reliable, the structure parameters of the circulator designed

in this paper are the same as the literature [18]. In Fig. 2, the radius of dielectric pillar is  $r_0 = 0.18a$ , with lattice constant  $a = 1.25\text{mm}$  and the background is air. The dielectric pillar array chose lower loss ceramics material such as  $\text{Al}_2\text{O}_3$  with refractive index  $n_0 = 3.4$  according to literature [19].

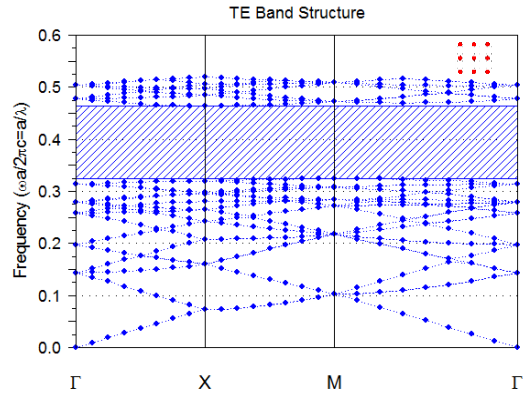


Fig. 4. Band gap for square lattice photonic crystals

The numerical results show that there is a wide photonic band gap in square lattice pillars array, which is expressed as normalized frequency range  $a/\lambda = 0.3265 \sim 0.4266$ , shown in Fig. 4, where  $c$  is speed of light. In this frequency range, electromagnetic waves will be limited to a stable transmission in the three line defect waveguides.

### 3.2. TE wave transmission in circulator

In Fig. 2, the MPC circulator is constituted by inserting a ferrite post in the center of the three line defect waveguides. Under the external magnetic field of  $H_0 = 3.2 \times 10^5 \text{ A/m}$  applied along z-direction in the center area, the transmission situation of TE wave was simulated by finite element method at center normalized frequency of  $a/\lambda = 0.4132$ , as shown in Fig. 5. The calculated region is divided into about 50 thousand grid cells with scattering boundary condition (SBC).

The simulated results show that the designed circulator has the function of turning on sequentially in forward direction but isolation in reverse direction, as shown in Fig. 5, where Port A, B, and C represent the three ports of the circulator. For example in Fig. 5(a), the doubly degenerate modes take place and coupling in the ferrite post under the external DC magnetic field, and the wave

front rotation an angle of  $90^\circ$ . Consequently, the TE wave incident from Port A is almost entirely transmitted to Port B (the output port) and isolating Port C (the isolated ports), similarly in Figs. 5(b)(c). And the corresponding amplitude of  $E_z$  field in 2D MPCs circulator are shown in Figs. 5(d)(e)(f), respectively.

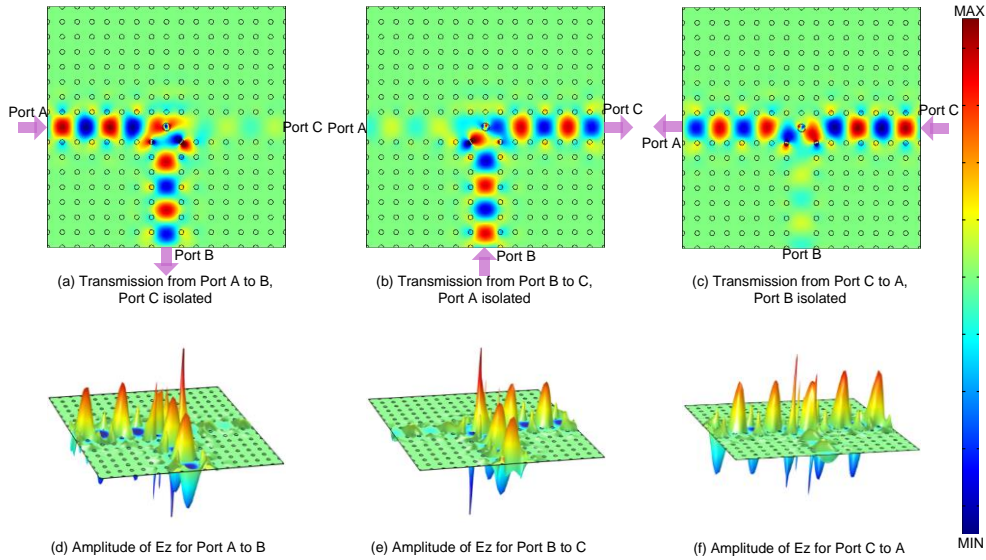


Fig. 5. (a-c)  $E_z$  field transmission in 2D MPC circulator; (d-f) Amplitude of  $E_z$  field in 2D MPC circulator

### 4. Discussion

#### 4.1. External characteristic parameters with frequency variation

In order to optimize the performance of the circulator, the external characteristic parameters of circulator are discussed by changing the frequency of incident TE wave. When TE wave is launched from one of the three ports (Port A, B, and C), the energy of output signal will be gathered at the other two ports. The circulator's isolation and insertion loss with frequency variation are calculated

by comparing the energy between the input port and output port, as shown in Fig. 6. The numerical results show that the isolation and insertion loss for the first two transmission paths of Figs. 5(a)(b) have a slightly different generally, as shown in Fig. 6(a). At the center frequency of  $a/\lambda = 0.4132$ , isolation and insertion loss reach maximum 24.36dB and minimum 0.081dB for Fig. 5(a); 25.17dB and 0.075dB for Fig. 5(b). When frequency diverges from the center frequency, the transmission characteristics of the circulator deteriorate gradually with increasing frequency offset.

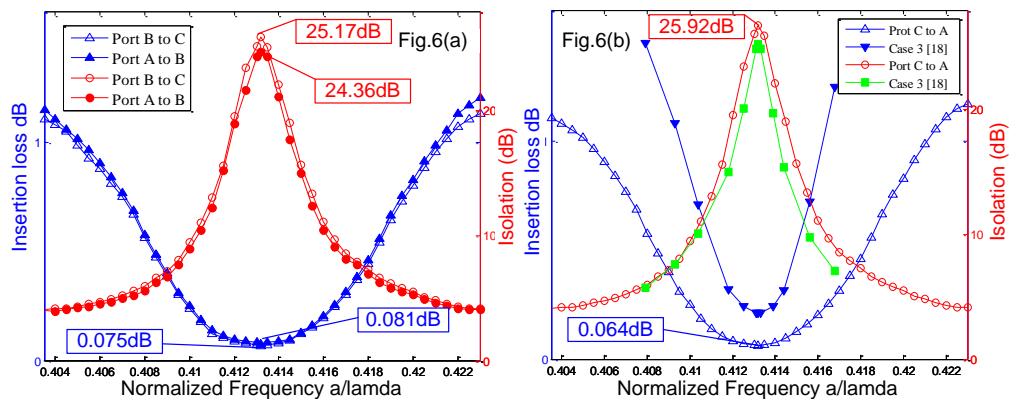


Fig. 6. External characteristics of the circulator: (a) Isolation and insertion loss for the first two transmission paths; (b) Isolation and insertion loss for the third path compared with those in literature [18]

An excellent coincidence is found by making a comparison of the overall variation trends of isolation and insertion loss with frequency in this article with those numerical results of corresponding literature [18], as shown in Fig. 6(b). Where, solid line of inverted triangle and square represent the insertion loss and isolation of literature [18] in the third transmission path, respectively. By comparing the peak value of isolation and insertion loss between our numerical results and [18], lower insertion loss of 0.064dB is obtained in our Fig. 2, the reason is that in [18] there are four ferrite posts and center defect pillar may bring more energy loss. The max of isolation 25.92dB for the third transmission path in this article also has a great improvement.

#### 4.2.3 cm T-shaped MPC circulator

Theoretically, the central frequency of the micro resonator is determined by the size of ferrite column and circulator can be obtained in different operating frequencies by flexibly changing the radius of the center ferrite post in the photonic band gap of  $a/\lambda=0.3265\sim 0.4266$ .

In the previous section, circulator is operating at

normalized frequency of  $a/\lambda = 0.4132$ , and the corresponding wavelength is about 27.23 mm. Thereby, it is need to slightly enlarge the radius  $r_2$  of the center ferrite post to realize a circulator with operating wavelength of 3 cm in this section, and corresponding normalized frequency is  $a/\lambda = 0.375$ .

The numerical result shown that, when the radius is increased to  $r_2 = 2.07 r_0$  and  $r_1 = 1.16 r_0$ , the circulator is operating at wavelength of 3 cm with the external DC magnetic field of  $H_0 = 3.5 \times 10^5 A/m$ . Electromagnetic field propagation in 2D MPC circulator is already discussed in section 3.2 and will not be repeated. Taking the third transmission path as an example, the TE wave has 5 peaks and 5 troughs for Fig. 5(f) but only 4 peaks and 4 troughs for Fig. 7(f) in the same size square lattice photonic crystal waveguide. It is obviously seen that wavelength in Figs. 7(a)(b)(c) is appreciably increscent compared with those of Figs. 5(a)(b)(d).

Complementary, we can also control the transmission direction of circulator by reversing the direction of the external magnetic field in order to realize two-way transmission, as shown in Fig. 7(g)(h). Since the symbol of off-diagonal element  $\kappa$  is decided by the direction of external DC magnetic field.

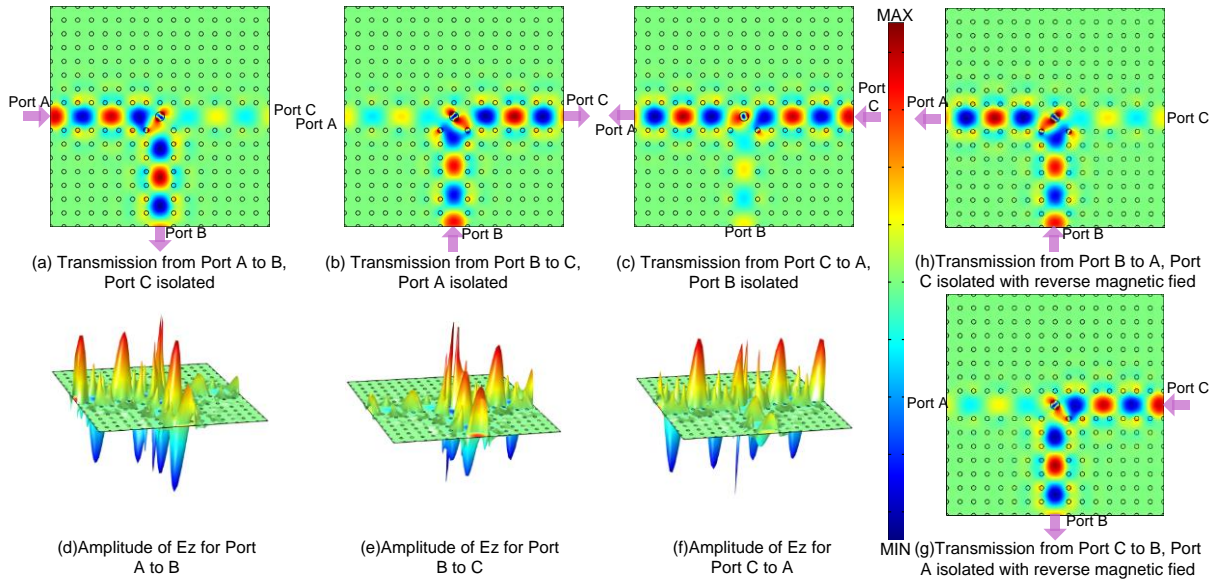


Fig. 7. (a-c)  $E_z$  field transmissions in 3cm T-shaped 2D MPC circulator; (d-f) Corresponding amplitude of  $E_z$  field in 2D MPC circulator, (g) Excited at Port C with reverse magnetic field; (h) Excited at Port B with reverse magnetic field

## 5. Conclusions

In summary, we research the gyromagnetic properties of an  $Al_2O_3$ -Ferrite MPC defect structure in the centimeter region. Based on Faraday gyromagnetic effect, a novel T-shaped waveguide circulator is considered by inserting gyromagnetic ferrite posts in photonic crystal pillar array. The excellent external characteristic parameters of isolation 25.92dB and inserting loss 0.064dB maybe provide a feasible method to develop an integrated

conveniently T-shaped circulator for large scale integrated optical circuit. As to the circulator it should be noted that, only one ferrite post in the waveguides acts as resonant cavity and provides enough Faraday rotation, so it can greatly reduce the insertion loss from multiple columns. At last but not the least, a 3 cm direction controllable circulator is obtained by precisely adjusting the radius of ferrite and reversing the direction of the external magnetic field.

### Acknowledgment

We thank the support from the National Natural Science Foundation of China (NSFC; grant 61171006).

### References

- [1] E. Yablonovitch, *Phys. Rev. Lett.* **58**, 2059 (1987).
- [2] S. John, *Phys. Rev. Lett.* **58**, 2486 (1987).
- [3] G. Shen, H. Tian, D. Yang, Y. Ji, *IEEE Photonics J.* **5**, 5501311 (2013).
- [4] J. G. Mutitu, S. Shi, A. Barnett, D. W. Prather, *IEEE Photonics J.* **2**, 490 (2010).
- [5] Q. Zhao, K. Cui, Z. Huang, X. Feng, D. Zhang, F. Liu, W. Zhang, Y. Huang, *IEEE Photonics J.* **5**, 2200606 (2013).
- [6] M. G. Scullion, T. F. Krauss, A. D. Falco, *IEEE Photonics J.* **3**, 203 (2011).
- [7] Q. Liu, Z. B. Ouyang, C. J. Wu, C. P. Liu, J. C. Wang, *Opt. Express* **16**, 18992 (2008).
- [8] J. Mao, J. Li, C. Zhou, H. Zhao, H. Sheng, *Laser Phys.* **23**, 54 (2013).
- [9] Y. Lian, G. Ren, B. Zhu, Y. Gao, W. Jian, W. Ren, S. Jian, *Laser Phys. Lett.* **14**, 055101 (2017).
- [10] Y. Cai, X. Chen, N. Li, C. Li, Y. Wang, *Laser Phys.* **27**, 035801 (2017).
- [11] Z. Wang, S. H. Fan, *Opt. Lett.* **15**, 1989 (2005).
- [12] F. Fan, S. J. Chang, C. Niu, Y. Hou, X. H. Wang, *Opt. Commun.* **285**, 3763 (2012).
- [13] Q. Wang, Z. B. Ouyang, *J. Opt. Soc. Am. B* **28**, 703 (2011).
- [14] S. H. Fan, Z. Wang, *J. Magnet. Soc. Jap.* **30**, 641 (2006).
- [15] Z. Wang, S. H. Fan, *Appl. Phys. B* **81**, 369 (2005).
- [16] A. A. Jalali, A. T. Friberg, *Opt. Lett.* **30**, 1213 (2005).
- [17] E. K. N. Yung, D. G. Zhang, R. S. K. Wong, *IEEE Trans. on Microwave Theory and Tech.* **44**, 454 (1996).
- [18] Q. Wang, Z. B. Ouyang, K. Tao, M. Lin, S. Ruan, *Physics Letters A* **376**(4), 646 (2012).
- [19] M. T. Sebastian, H. Jantunen, *International Mat. Rev.* **53**, 57 (2008).

\*Corresponding author: dgzhang@szu.edu.cn